ISBN: 978-3-95450-210-3 doi:10.18429/JACoW-FEL2019-TUP009

INTEGRATION OF AN XFELO AT THE EUROPEAN XFEL FACILITY*

P. Rauer†, I. Bahns, W. Hillert, J. Rossbach, Universität Hamburg , Hamburg, Germany
W. Decking, Deutsches Elektronen Synchrotron (DESY), Hamburg, Germany
Harald Sinn, European XFEL GmbH, Schenefeld, Germany

Abstract

An X-ray free-electron laser oscillator (XFELO) is a fourth generation X-ray source promising radiation with full three dimensional coherence, nearly constant pulse to pulse stability and more than an order of magnitude higher peak brilliance compared to SASE FELs. Proposed by *Kim et al.* in 2008[1] an XFELO follows the concept of circulating the light in an optical cavity - as known from FEL oscillators in longer wavelength regimes - but uses Bragg reflecting crystals instead of classical mirrors. With the new European X-ray free-electron laser (XFEL) facility recently gone into operation, the realization of an XFELO with radiation in the Angstrom regime seems feasible. Though, the high thermal load of the radiation on the cavity crystals, the high sensibility of the Bragg-reflection on reflection angle and crystal temperature as well as the very demanding tolerances of the at least 60 m long optical resonator path pose challenges which need to be considered. In this work these problems shall be summarized and results regarding the possible integration of an XFELO at the European XFEL facility will be presented.

INTRODUCTION

Current hard X-ray free-electron laser (FEL) facilities all use the self-amplified spontaneous emission (SASE) scheme for operation. While these sources produce very brilliant femtosecond X-ray pulses with excellent transverse coherence, they suffer from a lack of longitudinal coherence. A promising approach for reaching full longitudinal coherence in the hard X-ray regime proposed by *Kim et al.* in 2008 [1] is the X-ray free-electron-laser oscillator (XFELO). This scheme is based on using an undulator very short compared to state of the art hard X-ray SASE sources and a highly reflective cavity based on very pure diamond crystals serving as Bragg reflectors. As these Bragg reflectors also act as spectral filters an XFELO promises a spectral bandwidth in the order of the crystals bandwidth ($\Delta\lambda/\lambda_c \approx 10^{-5} - 10^{-7}$) and therefore orders of magnitude better than SASE-FELs. Furthermore, as the radiation field is built up over many cavity round trips, very low shot-to-shot fluctuations can be expected, even making the XFELO a promising candidate for X-ray quantum optics (XQO) [2]. With the recently commissioned European XFEL the realization of an XFELO becomes in reach. This is due to the facility's excellent electron beam properties and especially due to its very high bunch repetition rate of up to 4.5 MHz in pulsed-mode [3] which enables resonator lengths of only 33 m.

* Work supported by BMBF (FKZ 05K16GU4)
† patrick.rauer@desy.de

As will be evident from the following section, given the beam properties of the European XFEL the single pass gain exceeds a simple low gain oscillator, i.e. the case as discussed in the original proposition by *Kim et al.* in 2008. This comes with some advantages such as lower demands on the mechanical tolerances, but also with some disadvantages as will be discussed later.

A major issue one needs to address when dealing with an XFELO is the effect of the light-matter interaction between the X-ray field and the Bragg reflectors. This is due to the high requirements for the angular and spatial stability [4, 5] as well as the necessity of very stable Bragg conditions. In the following simulations excluding and including the effect of heating on the XFELO stability will be shown indicating a high relevance of appropriately handling heating effects.

XFELO WITHOUT HEAT LOAD

The simulations of an X-ray oscillator shown in this paper are all based on a combination of the established FEL code *Genesis1.3*[6] and a self written three dimensional wavefront propagation code which first transforms the radiation from the time into the frequency domain and then propagates each two dimensional frequency slice based on the *Fourier Optics* approach[7, 8]. The reflection of the radiation with the Bragg mirrors (in all three reciprocal dimensions) is currently evaluated based on the approximate two-beam dynamical diffraction theory[1].

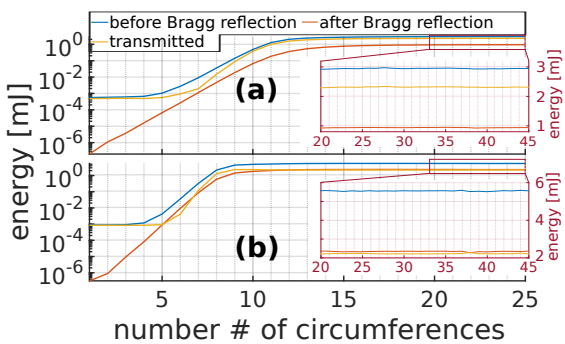

Figure 1: The pulse energy in logscale vs. number of circumferences after the undulator (blue), directly before reentering the undulator (red) and of the forward transmitted pulse (orange) for (a) 250 pC and (b) 500 pC electron bunches. The inset show the saturated energy curve in linear scale and extents the abscissa.

Figure 1 shows the simulation results based on a very simple two diamond mirror XFELO backscattering configuration[2] with one focusing lens. For out-coupling the downstream

[1] It will soon be extended by the more general n-beam diffraction theory.
[2] As such backscattering geometry induces multiple beam diffraction - not included in the simulations - an actually realized XFELO would be based on a more complex mirror setup.

ISBN: 978-3-95450-210-3 doi:10.18429/JACoW-FEL2019-TUP009

Table 1: Important Parameters Used for Simulation With the Slice Specific Parameters Given for the Slice with the Peak Current

	bunch charge	beam energy	energy spread	energy chirp	bunch length	peak current	norm. slice emittance	und. parameter
	q [pC]	E_B [GeV]	σ_E [MeV]	ΔE [MeV]	t_B [fs]	I_A[kA]	$\epsilon_{(x,y)}$ [mm mrad]	K_{Und}
(a)	250	14.5	0.5	17	24	5.05	(0.324,0.289)	2.8784
(b)	500	14.5	0.5	12	42	4.91	(0.364,0.338)	2.8685

und. length	avg. beta	Bragg wavelength	resonator length	focal length	angular jitter	t-jitter	mirror tilt	cavity loss factor
L_U [m]	$\bar{\beta}_{(x=y)}$ [m]	λ_c [Å]	L_{Cav} [m]	f_{Lense} [m]	$\tilde{\sigma}_k$ [nrad]	$\tilde{\sigma}_t$ [fs]	$\Delta\Theta$ [nrad]	R_{Cav}
20	25	1.3698	33.31	33.31	100	30	100	0.2

mirror is taken as only $t_{C1} = 42\,\mu$m thick having a transmission of 2.5 % at the resonant wavelength while the upstream one is taken as $t_{C2} = 150\,\mu$m. The simulations were calculated for realistic electron beam distributions produced by *Igor Zagarodnov et al.*[9] which were projected and parametrized to the longitudinal dimension with every slice of time containing information derived from the transverse dimensions. Additionally important error sources such as angular and timing jitter of the e-beam and mirror tilt are included. Other errors such as absorption in the idealized lenses are taken into account by using a cavity loss factor R_{Cav} describing the fraction of these losses compared to the total reflected energy. Table 1 displays important parameters of the electron distributions, the magnitude of the errors as well as other significant parameters related to the XFELO such as the undulator parameter K, the central reflection wavelength λ_c, and parameters related to the optical cavity configuration.

As Fig. 1 shows both the (a) 250 pC and the (b) 500 pC electron bunches saturate to quite high photon energies in the millijoule range in only few passes while having a bandwidth of only $\sigma_f \approx 10^{-5}$ and furthermore showing a very high stability on the energy range as can be seen from the inset. Still, there a some things to note. First, the (b) 500 pC case shows with $\mathcal{G} \approx 9$ a severely higher peak single pass gain $\mathcal{G}$ than the (a) 250 pC case with $\mathcal{G} \approx 3.5$, while for a SASE-FEL one would rather expect a comparable gain but saturation at roughly twice the pulse energy. The reason for that is the width of the electron bunches. As the temporal width of the reflected pulse is, due to the small spectral reflection bandwidth, roughly on the order of $t_R \approx 60$ fs the 500 pC electron beam has more overlap with the reflected and stretched seed and therefore also gets a higher gain. Another peculiar fact to note is the high transmitted energy which is $E_{trans}^{500\,\mathrm{pC}} = 2.22(1)$ mJ for the (b) 500 pC and even higher $E_{trans}^{250\,\mathrm{pC}} = 2.32(1)$ mJ for the (a) 250 pC bunches and therefore strongly exceeding the transmitted fraction of only a few percent noted before. The reason is the same as for the difference in gain. As due to the Fourier limit a 24 fs or a 42 fs long electron pulse will always generate a spectral width greater than the reflection bandwidth of the regarded (3 3 3)-diamond reflex, the spectral tails which are outside of this bandwidth will get transmitted width nearly 100 % as shown in Figs. 2(a) and 2(b). As the single pass gain for the regarded parameters is much higher than for a classical low gain FEL oscillator there is a considerable fraction of energy in these tails which leads to high transmitted energy but also a higher spectral width and quite peculiar spectral shape of the transmitted pulse. Also the energy jitter of the transmitted pulse is, with roughly a fraction of 10^{-2}, lower than for a SASE-FEL but higher than at a conventional FEL Oscillator(FELO) which averages the pulse energy over hundreds of round trips.

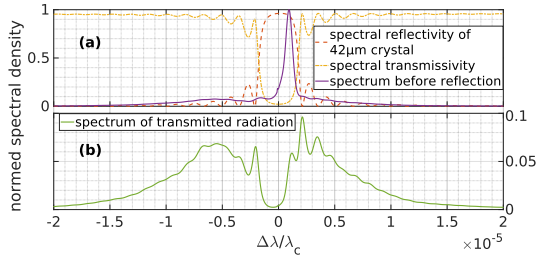

Figure 2: The spectra of the (a) saturated radiation pulse after the undulator before reflection and (b) the out coupled radiation of the 250 pC electron bunch. The majority of the transmitted energy lies in the tails of the incoming radiation outside the reflection bandwidth.

INFLUENCE OF HEAT LOAD

As can be seen from the results presented in Fig. 1 the pulse energy in a saturated XFELO can reach up to several millijoule. Even when taking into account a more conservative estimate of some hundreds of microjoule it is evident that at a rate of at some MHz this will lead to a considerable heat load on the crystal as was already shown by *Zemella et al.*[10]. Approximating the resonant wavelength λ_c with Bragg's law $\lambda_c \tilde{\propto} a_{lat}(T)$ being proportional to the lattice parameter $a_{lat}(T)$ one sees that it is very sensitive to the thermal expansion and therefore to the heat load. It has already been discussed[10] and shown[11] that cooling the crystal to 50 K or 100 K can ease this effect due to the reduced thermal expansion and the much increased thermal conductivity and would be of utter importance for XFELO operation.

As was discussed by *Maag et al.* in 2017[11] the very high phonon mean free path l_{mfp} in diamond reaching up to the mm-range at low T introduces effects which are not incorporated in the diffusive Fourier's law and effectively lower the scalar thermal conductivity κ_C, especially when one conservatively assumes purely diffusive scattering at the boundaries. In this work this is incorporated assuming radial symmetry and purely diffusive scattering by using a effective anisotropic thermal conductivity [12–14]

$$\vec{\kappa}_C^{\,\mathrm{eff}}(T) = \kappa_C^{\mathrm{bulk}}(T) \cdot \begin{pmatrix} \left[1 + 4/3 \cdot l_{\mathrm{mfp}}^{\mathrm{bulk}}(T)/t_{\mathrm{C}}\right]^{-1} \\ \left[1 + 3/8 \cdot l_{\mathrm{mfp}}^{\mathrm{bulk}}(T)/t_{\mathrm{C}}\right]^{-1} \end{pmatrix}$$

ISBN: 978-3-95450-210-3 doi:10.18429/JACoW-FEL2019-TUP009

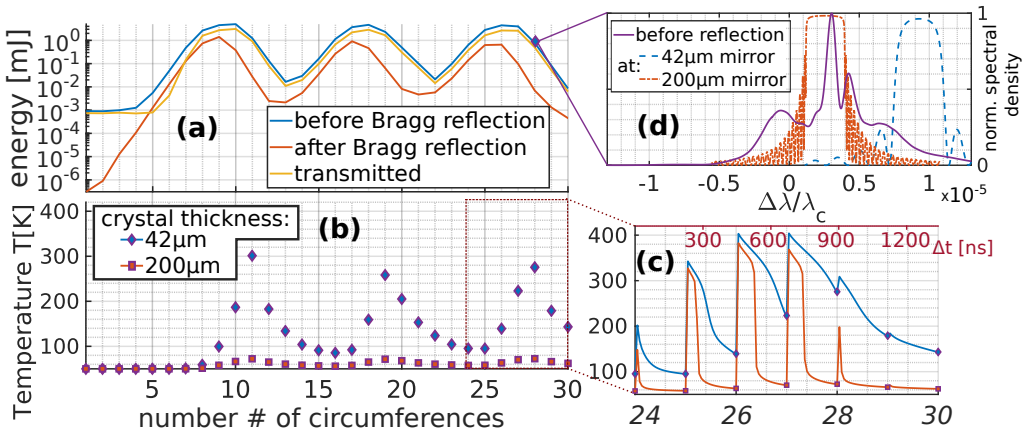

Figure 3: Simulation results of the 500 pC electron bunch with parameters denoted in table 1 but including the influence of the heat load on the crystal temperature. (a) shows the energy vs the number of circumferences clearly exhibiting strong oscillatory features. (b) shows the crystal surface temperature at the center of the incoming beam at the arrival of the next pulse important for the reflection while (c) shows the actual temperature progression also in between the pulses exemplary for the last few passes. Figure (d) shows the spectrum of the radiation after the undulator at the exemplary circumference #28 where the energy peaks and the strongly shifted reflection curves.

with the first dimension being the cross plane and the second dimension the in plane (radial) thermal conductivity.

Figure 3 shows the results for the parameters of the 500 pC electron beam from table 1 but this time including the influence of heat load which was simulated using the FEM-software *COMSOL Multiphysics®*. Despite starting from $T_{crys} = 50$ K Fig. 3(a) shows a strong effect on the energy curve. While showing peak energies comparable to or, for the transmitted beam with $E_{trans}^{500\,\mathrm{pC}} = 3.1$ mJ, even slightly higher than the case without heat load, the energy drops significantly after the peak and show a oscillatory behavior. These particular features can be explained by looking at the temperature T at the photon pulse arrival time displayed in 3(b) and the exemplary spectrum shown in 3(d) for the 28^{th} circumference. The first thing to note is that the energy does not mainly drop due to the overall shift of the reflection curves with respect to the base resonant wavelength λ_c but due to the larger shift of the thin out-coupling diamond with respect to the thick diamond's reflection curve. This leads to a combined reflectivity of only few %. As can be seen from the temperature curves the thin diamond heats significantly more than the thick diamond which is not only due to the effective thermal conductivity reduction discussed above but also due to the smaller volume where the heat can diffuse to. This is also evident from looking at Fig. 3(c) exhibiting much slower thermal diffusion in the thin diamond after circumference #27 even though starting at nearly the same peak temperature. This points out that the entire crystal volume close to the interaction area with the X-ray pulse is at an elevated temperature reducing the temperature gradient ∇T and therefore thermal diffusion.

The reason for the flatness of the peaks is mainly due the high gain of $\mathcal{G} \approx 9$ compensating reflection losses caused by the resonant wavelength shifts. That allows the heat to build up over - in this case - around three round trips until it leads to the situation depicted in Fig. 3(d) having reflection losses which cannot be compensated by the gain anymore. Then it takes another some five round trips with low incoming radiation energy for the heat to dissipate in the crystal and the two reflection curves reach enough overlap to allow effective pass-to-pass gain greater than zero.

DISCUSSION AND OUTLOOK

Based on the results shown in **XFELO WITHOUT HEAT LOAD** which were obtained by using realistic electron beams optimized for standard SASE operation with strong chirp and critical error sources such as angular beam jitter and mirror tilt the realization of an XFELO seems very feasible at the European XFEL. Even assuming higher cavity losses one would still reach an out-coupled beam with a brilliance higher than any available SASE source while showing a very good shot to shot stability. Unfortunately this view changes when taking into account the effect of heat load on the crystal temperature as shown in the previous section. This still allows high peak brilliance but the out-coupled beam would show severe shot to shot jitter. Nonetheless there are some possibilities to handle the effect. The simplest would be to lower the single pass gain leading to reduced saturation energies and bringing the XFELO more closely to the operation of a conventional FELO. Another possibility is to use a thicker out-coupling mirror reducing the strong shift of the reflection curves with respect to each other. This would be possible due to the short electron bunches producing spectra wider than the diamond reflection width. This comes with the cost of an out-coupled radiation more subject to shot to shot jitter in the electron parameters but which is mostly compensated by the strong single mode coherent seeding.

Finally, tests at the European XFEL are considered.

ACKNOWLEDGEMENTS

This research was supported in part through the Maxwell computational resources operated at Deutsches Elektronen-Synchrotron (DESY), Hamburg, Germany.

ISBN: 978-3-95450-210-3 doi:10.18429/JACoW-FEL2019-TUP009

REFERENCES

[1] K.-J. Kim, Y. Shvyd'ko, and S. Reiche, "A proposal for an x-ray free-electron laser oscillator with an energy-recovery linac," *Physical Review Letters*, vol. 100, no. 24, Jun. 2008. DOI: 10.1103/physrevlett.100.244802.

[2] B. Adams and K.-J. Kim, "X-ray comb generation from nuclear-resonance-stabilized x-ray free-electron laser oscillator for fundamental physics and precision metrology," *Physical Review Special Topics - Accelerators and Beams*, vol. 18, no. 3, Mar. 2015. DOI: 10.1103/physrevstab.18.030711

[3] *European XFEL*, http://www.xfel.eu/overview/facts_and_figures/

[4] S. Stoupin, F. Lenkszus, R. Laird, K. Goetze, K.-J. Kim, and Y. Shvyd'ko, "Nanoradian angular stabilization of x-ray optical components," *Review of Scientific Instruments*, vol. 81, no. 5, p. 055 108, 2010. DOI: http://dx.doi.org/10.1063/1.3428722

[5] C. Maag, J. Zemella, and G. J. Rossbach, "Numerical studies of the influence of the electron bunch arrival time jitter on the gain process of an xfel-oscillator for the european xfel," in *Proc. of FEL2015, Daejon, Korea*, paper TUP032, 2015, pp. 436–438.

[6] S. Reiche, *Genesis 1.3,* http://genesis.web.psi.ch/

[7] O. Chubar, M.-E. Couprie, M. Labat, G. Lambert, F. Polack, and O. Tcherbakoff, "Time-dependent FEL wavefront propagation calculations: Fourier optics approach," *Nuclear Instruments and Methods in Physics Research Section A: Accelerators, Spectrometers, Detectors and Associated Equipment*, vol. 593, no. 1-2, pp. 30–34, Aug. 2008. DOI: 10.1016/j.nima.2008.04.058

[8] J. D. Schmidt, *Numerical Simulation of Optical Wave Propagation With Examples in MATLAB*, ser. SPIE Press Monograph. SPIE Press, 2010, vol. Vol. PM199, ISBN: 978-0-8194-8326-3

[9] I. Zagorodnov, "Start2end simulation fel beam xfel," 2014, http://www.desy.de/fel-beam/s2e/xfel.html

[10] J. Zemella, J. Rossbach, C. Maag, M. Tolkiehn, and H. Sinn, "Numerical simulations of an XFELO for the European XFEL driven by a spent beam," in *Proc. of FEL2012, Nara, Japan*, paper WEPD29, 2012, pp. 429–433, ISBN: 978-3-95450-123-6.

[11] C. Maag, I. Bahns, J. Rossbach, and P. Thiessen, "An experimental setup for probing the thermal properties of diamond regarding its use in an xfelo," in *Proc. of FEL2017, Santa Fe, USA*, paper MOP064, 2017, pp. 200–203. DOI: 10.18429/JACoW-FEL2017-MOP064

[12] A. Majumdar, "Microscale heat conduction in dielectric thin films," *Journal of Heat Transfer*, vol. 115, no. 1, p. 7, 1993. DOI: 10.1115/1.2910673

[13] J. Maassen and M. Lundstrom, "Steady-state heat transport: Ballistic-to-diffusive with fourier's law," *Journal of Applied Physics*, vol. 117, no. 3, p. 035 104, 2015. DOI: 10.1063/1.4905590

[14] J. Kaiser, T. Feng, J. Maassen, X. Wang, X. Ruan, and M. Lundstrom, "Thermal transport at the nanoscale: A fourier's law vs. phonon boltzmann equation study," *Journal of Applied Physics*, vol. 121, no. 4, p. 044 302, Jan. 2017. DOI: 10.1063/1.4974872